Master stability analysis in transient spatiotemporal chaos

Renate Wackerbauer*
Department of Physics, University of Alaska, Fairbanks, Alaska 99775-5920, USA
(Received 15 August 2007; published 9 November 2007)

The asymptotic stability of spatiotemporal chaos is difficult to determine, since transient spatiotemporal chaos may be extremely long lived. A master stability analysis reveals that the asymptotic state of transient spatiotemporal chaos in the Gray-Scott system and in the Bär-Eiswirth system is characterized by negative transverse Lyapunov exponents on the attractor of the invariant synchronization manifold. The average lifetime of transient spatiotemporal chaos depends on the number of transverse directions that are unstable along a typical excitation cycle.

DOI: 10.1103/PhysRevE.76.056207 PACS number(s): 05.45.Jn, 05.45.Xt

I. INTRODUCTION

Transient spatiotemporal chaos is a generic pattern in extended nonequilibrium systems; spatiotemporal dynamics changes spontaneously from chaotic to regular (steady state or periodic) behavior without external influence. Turbulence in shear flow is reported to be transient [1]; in models, spatiotemporal chaos was found to be transient in semiconductor charge transport [2], in CO oxidation on single-crystal Pt surfaces [3], in a cubic autocatalytic reaction [4], in turbulent dynamics [5,6], and in systems of coupled logistic maps [7,8]. "Stable chaos" (with a positive Lyapunov exponent) is transient in systems of coupled one-dimensional maps [9,10]. Transient spatiotemporal chaos was also discussed as a mechanism for species extinction in ecology [11,12].

The asymptotic stability of chaotic dynamics in extended systems is difficult to determine, since transient spatiotemporal chaos may be extremely long lived; its average lifetime typically increases exponentially with the size of the medium [2–4,6,10,13] or with the Reynolds number in shear flow [1]. Noise and nonlocal coupling may further influence the collapse process in realistic systems, which enhances the difficulties in determining the asymptotic stability. For transient chaos in the Gray-Scott reaction-diffusion network, noise could clearly delay or advance the collapse [14], and the addition of two or more nonlocal couplings to a ring network could make transient spatiotemporal chaos asymptotic [15].

In contrast to low-dimensional systems where a chaotic repellor is known to govern transient chaos [16], the mechanistic understanding of the collapse in extended systems remains elusive. In the Gray-Scott model [17] and in the Bär-Eiswirth model [18] the sudden collapse of spatiotemporal chaos is initiated by a high degree of synchrony in the regular ring network [4]. The master stability function [19,20] quantifies synchronization stability of linearly coupled dynamical elements. This paper explores for two models whether the master stability function, which quantifies the stability of transverse perturbations close to the synchronization manifold, is a good indicator for transient vs asymptotic spatiotemporal chaos. The two models, a ring network of Gray-Scott excitable elements and a ring network of Bär-Eiswirth excitable elements, are introduced in Sec. II and their transient dynamics discussed. In Sec. III the master stability analysis is applied, and in Sec. IV relations of transient lifetime and unstable transverse directions are discussed in numerical simulations.

II. TRANSIENT SPATIOTEMPORAL CHAOS IN RING NETWORKS

The ring network consists of N diffusively coupled, identical, continuous-time dynamical elements. At each network node $n(n=1,2,\ldots N)$ the uncoupled dynamics is given by $\frac{d\mathbf{x}_n}{dt}=\mathbf{F}(\mathbf{x}_n)$ with $\mathbf{x}_n$ a d-dimensional state vector. The coupled dynamical system [19] is given by

$$\frac{d\mathbf{x}_n}{dt}=\mathbf{F}(\mathbf{x}_n)+\sigma\sum_{j=1}^{N}G_{nj}H(\mathbf{x}_j). \tag{1}$$

σ determines the global strength of the coupling. $H:R^d\to R^d$ is a coupling function and G is a $N\times N$ symmetric Laplacian matrix ($\Sigma_{j=1}^{N}G_{ij}=0$) with following nonzero elements on the ring network: $G_{ii}=-2$ and $G_{i,i+1}=G_{i-1,i}=1$.

A. Ring network of excitable Gray-Scott dynamical elements

The two-variable ($d=2$) Gray-Scott (GS) model [21] describes an open, autocatalytic reaction: $A+2B\to 3B$ and $B\to C$. A represents the resource, B is the autocatalytic species, and C is the final product. From the regular diffusive coupling in both components, the coupling function in Eq. (1) becomes $H(\mathbf{x}_j)=\mathbf{x}_j$ with $\mathbf{x}_j=(a_j,b_j)^T$ and a_j and b_j the dimensionless concentrations of resource A and species B at node j. For the Gray-Scott dynamics Eq. (1) becomes (in dimensionless form)

$$\frac{da_n}{dt}=1-a_n-\mu a_n b_n^2+\sigma\sum_{j=1}^{N}G_{nj}a_j,$$

$$\frac{db_n}{dt}=\mu a_n b_n^2-\Phi b_n+\sigma\sum_{j=1}^{N}G_{nj}b_j. \tag{2}$$

Φ and μ are the bifurcation parameters, determined by the rate constants and the reactant concentration in the reservoir.

*ffraw1@uaf.edu

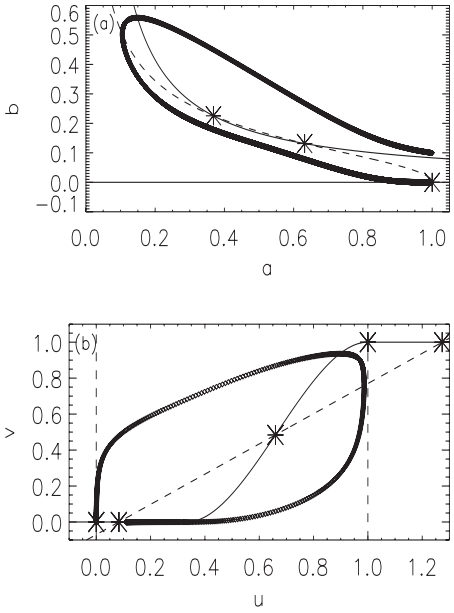

FIG. 1. Phase space diagram with steady states for the uncoupled GS dynamics (a) and for the uncoupled BE dynamics (b). The broad line marks a typical excitation cycle that ends at the stable rest state of the uncoupled system. The dashed (full) lines mark the nullclines corresponding to the first (second) component in the model equations. All the other parameters are the same as in Fig. 2.

In the absence of coupling [$\sigma=0$ in Eq. (2)], the dynamics is characterized by three steady states, $S^n=(1,0)$, $S^f=\left(\frac{1-\sqrt{1-4\Phi^2/\mu}}{2},\frac{1+\sqrt{1-4\Phi^2/\mu}}{2\Phi}\right)$, and $S^s=\left(\frac{1+\sqrt{1-4\Phi^2/\mu}}{2},\frac{1-\sqrt{1-4\Phi^2/\mu}}{2\Phi}\right)$. Linear stability analysis shows that S^n is a stable node for all parameter values μ and Φ. S^f is an unstable focus, and S^s is a saddle point, which exists for μ above the saddle node bifurcation point, $\mu_{sn}=4\Phi^2$. In the range $2<\Phi<4$, S^f becomes a stable focus above the subcritical Hopf bifurcation point, $\mu_H=\Phi^4/(\Phi-1)$. In the parameter regime of interest $[\mu_{sn},\mu_H]$ and $\Phi=2.8$ the dynamical system at each node is excitable. Figure 1(a) shows a typical excitation cycle in phase space together with the three steady states and the nullclines.

Earlier studies have shown that spatiotemporal chaos on a regular ring network [Eq. (2)] is transient [4]. After a regime of sustained spatiotemporal chaos with a rapid decay of spatial correlations and a positive largest Lyapunov exponent, the system exhibits a spontaneous, intrinsic collapse to the homogeneous stable steady state S^n with extinct species [Fig. 2(a)]. The average lifetime of transient spatiotemporal chaos increases exponentially with the size of the network N (Fig. 3). During the transient phase the spatiotemporally chaotic dynamics was characterized by a Šilnikov-like orbit that consists of a heteroclinic connection from the unstable focus S^f to the stable node S^n in the homogeneous system and a heteroclinic connection from S^n to S^f for the traveling wave system [17,23]. A typical trajectory at a network node spirals away from the unstable focus toward the stable node, only to be reinjected to the unstable focus via the propagating reaction-diffusion activity. The parameter range $[\mu_c,\mu_H]$ for wave-induced spatiotemporal chaos is determined by the

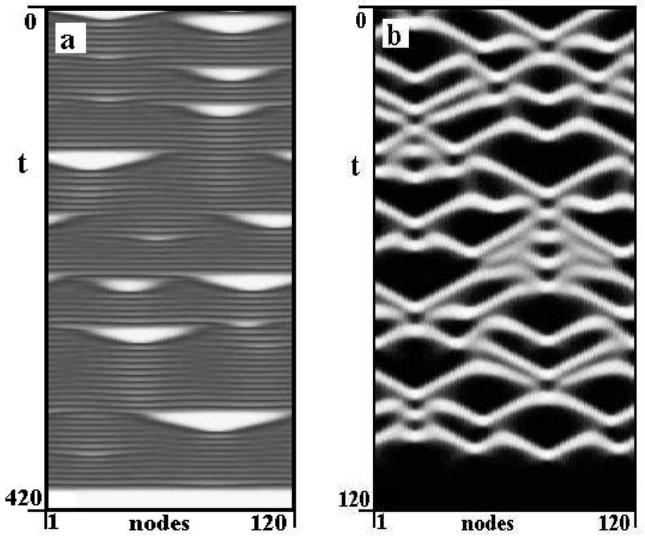

FIG. 2. Transient spatiotemporal chaos in (a) the Gray-Scott model [concentration a with $\mu=33.7$, $\Phi=2.8$, $N=120$, and $\sigma=16$ in Eq. (2) [4,22]], and (b) the Bär-Eiswirth model [concentration u with $\alpha=0.84$, $\beta=0.07$, $\epsilon=0.12$, $N=200$, and $\sigma=16$ in Eq. (3)]. The transient lifetime is $T=401$ (a) and $T=105$ (b). An explicit Euler method with a time step of $dt=0.0003$ was used for the numerical integration.

critical threshold for traveling wave solutions μ_c and the Hopf bifurcation point μ_H, with $\mu_c\approx 33$ for $\Phi=2.8$ [17].

The spatiotemporal pattern during the transient phase is characterized by an irregular distribution of local extinct regions [Fig. 2(a)], in which trajectories of neighboring network nodes approach the stable steady state S^n of the homogeneous system together [17]. The triangular shape of these local extinctions, where species B is extinct ($b=0$) and resource A recovers to its maximum value ($a=1$), is due to the propagation of species B into these regions of high resource concentration A from both sides. The collapse of spatiotemporal chaos is preceded by a quasihomogeneous spatial state (basin for immediate extinction in [4]) in which the perturbations that normally initiate reaction-diffusion fronts and

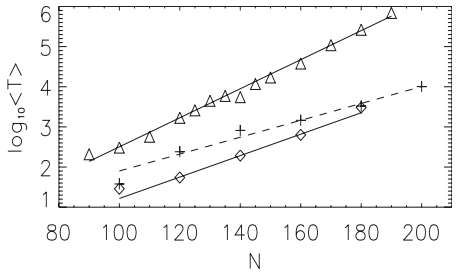

FIG. 3. Average transient lifetime $\langle T\rangle$ versus number of network nodes N for the Gray-Scott model [$\sigma=16(\triangle)$ and $\sigma=30(\diamond)$] and for the Bär-Eiswirth model [$\sigma=16(+)$]. Each data point was determined from 100 random initial conditions [24,25]. The error bar (one standard deviation, not plotted here) for each data point is of the order of $\langle T\rangle$ [26]. The lines show "robust least absolute deviation" fits of the average transient lifetimes (full line: GS model; dashed line: BE model). All the other parameters and simulation procedures are the same as in Fig. 2.

thus sustain spatiotemporal chaos are subthreshold. The trajectories throughout the network follow closely the heteroclinic connection from the unstable focus to the stable node, and the system reaches its stable, spatially homogeneous asymptotic state.

B. Ring network of excitable Bär-Eiswirth dynamical elements

The two-variable ($d=2$) Bär-Eiswirth (BE) model [18] describes a realistic surface reaction model for the oxidation of CO on Pt, with u an activator concentration and v an inhibitor concentration. Diffusive coupling is relevant only for the activator [18], which results in $H(u_j,v_j)=(u_j,0)$ for the coupling function in Eq. (1) when $\mathbf{x}_j=(u_j,v_j)^T$. For the Bär-Eiswirth model Eq. (1) becomes (in dimensionless form)

$$\frac{du_n}{dt}=\frac{1}{\epsilon}u_n(1-u_n)\left(u_n-\frac{v_n+\beta}{\alpha}\right)+\sigma\sum_{j=1}^{N}G_{nj}u_j,$$

$$\frac{dv_n}{dt}=f(u_n)-v_n \tag{3}$$

with

$$f(u)=\begin{cases}0, & u\le 1/3\\ 1-6.75u(u-1)^2, & 1/3\le u\le 1\\ 1, & u>1\end{cases}.$$

The function $f(u)$ yields a delayed inhibitor production unless $u<1/3$. α, β, and ϵ are bifurcation parameters, with ϵ determining the differences in the time scales for the slow variable v and the fast variable u.

For the uncoupled system [$\sigma=0$ in Eq. (3)], the dynamics is characterized by three steady states, a stable node $S^n=(0,0)$, a saddle point at $S^s=(\frac{\beta}{\alpha},0)$, and an unstable focus S^f to be calculated numerically. Two additional steady states, a saddle point at (1,1) and a stable node at $(\frac{1+\beta}{\alpha},1)$, are not relevant for the excitation cycle and for the regime in phase space ($u<1$) where spatiotemporal chaos exists. Figure 1(b) shows a typical excitation cycle in phase space together with the five steady states and the nullclines.

Spatiotemporal chaos in the BE model for a one-dimensional medium is discussed in [27]. For a typical parameter $\alpha=0.84$ and $\beta=0.07$ the traveling pulses become unstable for ϵ above a critical value $\epsilon_c=0.107$ to allow reexcitation behind the pulse to create new pulses. This backfiring instability is the origin of spatiotemporal chaos. With further increasing ϵ a saddle-loop bifurcation creates a stable limit cycle around the unstable focus until this limit cycle vanishes via a Hopf bifurcation to yield a bistable system. The Lyapunov exponent was found to be positive [27]. Strain and Greenside report for the two-dimensional system that spatiotemporal chaos is transient in the BE model [3]. They find that the average lifetime increases exponentially with the size of the medium.

Figure 2(b) shows a typical spatiotemporal pattern for transient spatiotemporal chaos in the BE system. This sudden collapse of spatiotemporal chaos to the homogeneous stable steady state with vanishing activator and vanishing inhibitor is similar to the GS system: The collapse is preceded by a quasihomogeneous spatial state, and the average transient lifetime increases exponentially with the network size N (Fig. 3). The spatiotemporal pattern during the transient phase is characterized by an irregular zigzag pattern [Fig. 2(b)]. Within the black triangular structures trajectories of neighboring network nodes approach the stable steady state of the homogeneous system together, which is in comparison to the white triangular patches for the GS system [Fig. 2(a)]. A typical trajectory at a network node spirals away from the unstable focus toward the stable node, only to be excited again by the propagating pulses.

III. MASTER STABILITY ANALYSIS

The synchronization manifold for Eq. (1) is given by $\mathbf{x}_n=\mathbf{x}$, $\forall n=1,2,\ldots,N$ with $\mathbf{x}$ a solution of the uncoupled system $\frac{d\mathbf{x}}{dt}=\mathbf{F}(\mathbf{x})$; an infinitesimal perturbation from the synchronous state, $\delta_n=\mathbf{x}_n-\mathbf{x}$, evolves according to [19]

$$\dot{\delta}_n=D\mathbf{F}(\mathbf{x})\delta_n+\sigma\sum_j G_{nj}DH(\mathbf{x})\delta_j. \tag{4}$$

The $d\cdot N$-dimensional vector $\delta=(\delta_1,\delta_2,\ldots,\delta_N)^T$ then follows:

$$\dot{\delta}=[1_N\otimes D\mathbf{F}(\mathbf{x})+\sigma G\otimes DH(\mathbf{x})]\delta \tag{5}$$

with 1_N representing the N-dimensional unit matrix. This variational equation can be block diagonalized,

$$S\otimes 1_d[1_N\otimes D\mathbf{F}(\mathbf{x})+\sigma G\otimes DH(\mathbf{x})](S\otimes 1_d)^{-1}$$
$$=1_N\otimes D\mathbf{F}+\sigma G_{\mathrm{diag}}\otimes DH,$$

if $SGS^{-1}=G_{\mathrm{diag}}=\mathrm{diag}(\lambda_0,\ldots,\lambda_{N-1})$. In the new coordinates, the block diagonal variational equations (master stability equation [19]) reads

$$\dot{\delta}_k=[D\mathbf{F}(\mathbf{x})+\sigma\lambda_k DH(\mathbf{x})]\delta_k,\qquad \forall\, k=0,1,\ldots,N-1. \tag{6}$$

λ_i are the eigenvalues of the coupling matrix G. For a symmetric coupling matrix G of the form $\Sigma_j G_{ij}=0$, the synchronization manifold is always a solution to Eq. (1), and $\lambda_0=0$ is always an eigenvalue of G with eigenvector $(1,1,\ldots,1)^T$. Since Eq. (6) represents the variational equation for the uncoupled system for $\lambda_0=0$, the corresponding Lyapunov exponents determine the stability within the synchronization manifold. The $d(N-1)$ remaining eigenvectors span the subspace transverse to the synchronization manifold. The variations (perturbations) transverse to the synchronization manifold [$\delta_i, i>0$, Eq. (6)] determine the stability of the synchronous state. The transverse stability is often quantified with the maximum Lyapunov exponent [19,28].

This master stability analysis is applied to transient spatiotemporal chaos in the GS model [Eq. (2)] and the BE model [Eq. (3)]. An invariant synchronization manifold exists for both systems, such that if all concentrations are equal at time $t=0$, then they are equal for all $t>0$.

For the GS system the master stability equation follows from Eq. (6) using $H=\mathbf{x}$ and $DH=1_2$. Since the attractor on the synchronization manifold is the stable node (1,0), the master stability equation becomes

$$\dot{\delta}_k = \begin{pmatrix} \sigma\lambda_k - \Phi & 0 \\ 0 & \sigma\lambda_k - 1 \end{pmatrix} \delta_k$$

with $k=1,\ldots,N-1$ for the transverse directions, and with $\lambda_k=-4\sin^2(k\pi/N)$ [19]. The $2(N-1)$ Lyapunov exponents, $\sigma\lambda_k-\Phi$ and $\sigma\lambda_k-1$, are all negative, and the synchronization manifold is attractive. Consequently, we expect the system to reach the attractor of the synchronization manifold and therefore transient spatiotemporal chaos. The maximum finite time Lyapunov exponent along the excitation cycle is negative too.

For the BE system the attractor on the synchronization manifold is the stable node (0,0). The master stability equation becomes

$$\dot{\delta}_k = \begin{pmatrix} \sigma\lambda_k - \dfrac{\beta}{\alpha\epsilon} & 0 \\ 0 & -1 \end{pmatrix} \delta_k$$

using $H(u,v)=(u,0)$ and $DH(u,v)=E=\mathrm{diag}(1,0)$. The Lyapunov exponents for all transverse modes k, with $k=1,2,\ldots,N-1$ are negative. The value of $N-1$ Lyapunov exponents is -1, and the other $N-1$ Lyapunov exponents are $\sigma\lambda_k-\frac{\beta}{\alpha\epsilon}$ with $\lambda_k=-4\sin^2(k\pi/N)$. Since the synchronization manifold is attractive, we expect a finite lifetime of spatiotemporal chaos, if the system reaches the neighborhood of the synchronization manifold.

IV. STABILITY OF TRANSVERSE MODES ALONG EXCITATION CYCLE

In the GS model and the BE model all the Lyapunov exponents on the attractor (i.e., point attractor) of the synchronization manifold are negative, which results in contraction transverse to the synchronization manifold everywhere on the attractor. Consequently, spatiotemporal chaos is transient. The maximum finite time Lyapunov exponent is negative along a typical excitation cycle, which is a trajectory within the synchronization manifold that is not restricted to the attractor. Although the synchronization manifold is attractive on average along the excitation cycle, some of the transverse modes are unstable somewhere along the excitation cycle. The number of transverse modes increases with the network size N, and the average lifetime of transient spatiotemporal chaos usually increases exponentially with N (Fig. 3). In the following we discuss how the number of unstable directions along the excitation cycle increases with N.

Each block k in the master stability equation [Eq. (6)] differs only by the eigenvalues λ_k of the coupling matrix. The coupling in the GS model [Eq. (2)] and in the BE model [Eq. (3)] is Laplacian, for which $\lambda_k=-4\sin^2(k\pi/N)$ [19]. The network size N only enters into λ_k. With $\kappa=k/N$ the master stability equation [Eq. (6)] becomes

$$\dot{\delta}_k = [D\mathbf{F}(\mathbf{x}) - 4\sigma\sin^2(\kappa\pi)DH(\mathbf{x})]\delta_k. \quad (7)$$

κ is treated as a continuous variable to facilitate the study of the transverse stability properties for all network sizes N. $\mathbf{x}$ represents the excitation cycle, a solution of the uncoupled system.

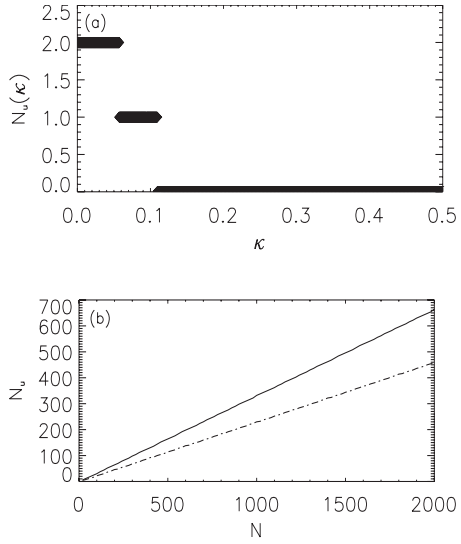

FIG. 4. (a) Maximum number of unstable directions $N_u(\kappa)$ along the excitation cycle for the transverse mode $\kappa=k/N$ in the GS model. Due to the symmetry of the eigenvalues of the Laplacian coupling matrix, $\lambda_k=\lambda_{N-k}$, only $\kappa\leq 0.5$ is plotted. (b) Total number of unstable transverse directions N_u vs network size N in the $2(N-1)$-dimensional transverse subspace of the GS model. The full line corresponds to the total number of directions that are unstable somewhere along the excitation cycle, $N_u=\Sigma_{k=1}^{N-1}N_u(\kappa)$. The dashed line corresponds to the maximum number of unstable directions at a point along the excitation cycle. All the other parameters and simulation procedures are the same as in Fig. 2(a).

A. Transverse modes in the GS model

Figure 4(a) shows which of the transverse modes can be unstable somewhere along the excitation cycle. For the GS system we find that the modes with smaller κ always correspond to two unstable directions, $N_u(\kappa)=2$. At an intermediate range of κ, only one direction is unstable somewhere along the excitation cycle, and with further increasing κ,all directions are stable everywhere along the excitation cycle $[N_u(\kappa)=0]$. The steplike pattern in Fig. 4(a) is robust to variations of the coupling strength σ, except that the intervals with $N_u(\kappa)>0$ increase with decreasing σ.

From Fig. 4(a) the total number of directions N_u that are transverse to the synchronization manifold and that are unstable somewhere along the excitation cycle is determined, $N_u=\Sigma_{k=1}^{N-1}N_u(\kappa)$. Figure 4(b) shows that the total number of unstable transverse directions increases linearly with the network size N. When calculating the number of unstable transverse directions of an individual point and taking the supremum over all points along the excitation cycle, the total number of unstable directions also increases linearly with the network size, as indicated by the dashed line in Fig. 4(b). The rate at which the total number of transverse directions that are unstable somewhere along the excitation cycle grows with the network size N is larger then the rate at which the maximum number of transverse directions that are unstable

at a point along the excitation cycle. Both rates dN_u/dN, however, do not fit the rate dT/dN at which the average lifetime of spatiotemporal chaos increases with N, particularly since $dT/dN=\gamma T$ and $dN_u/dN=\eta$ with γ, η positive real constants. For a given coupling strength σ, γ refers to the slope in Fig. 3, and η refers to the slope in Fig. 4(b).

A more detailed analysis of η and γ for various coupling strengths σ reveals that $\eta \neq \gamma$ and that η/γ depends on the coupling strength σ. Within a range of coupling strengths between $\sigma=15$ and $\sigma=30$ the value of η/γ is rather constant, and fluctuates about its mean value 9.34 with a standard deviation of 0.60 when η refers to the number of unstable directions somewhere along the excitation cycle; η/γ fluctuates about its mean value 6.40 with a standard deviation of 0.41 when η refers to the number of unstable directions at a point along the excitation cycle. For larger coupling strength (approximately $\sigma \geq 40$ in the simulations considered) η/γ clearly increases with σ, since then η varies only slowly with σ and γ decreases with σ.

The rate γT at which the average lifetime increases with the network size N is not quantitatively related in a simple way to the rate η at which the number of unstable transverse directions to the synchronization manifold increases with N. Qualitatively, however, γ (Fig. 3) and η decrease with increasing coupling strength σ such that the exponential growth of the average lifetime with the network size is reduced as is the growth rate of unstable transverse directions with the network size.

Figure 5(a) shows that the average lifetime of spatiotemporal chaos decreases with increasing coupling strength for a fixed network size N. This is consistent with earlier studies [4,14] insofar as the spatiotemporal pattern for weaker coupling strength has smaller but more local extinctions, whereas for strong coupling the typical size of a local extinction is clearly increased. Larger local extinctions make it more likely for the system to generate an extinction of the size of the network, i.e., a global collapse of spatiotemporal chaos. More local extinctions per unit time hinder the collapse of spatiotemporal chaos since the presence of a local extinction does not allow the system to become globally extinct. This is due to superthreshold perturbations of the stable node that are provided by the boundary of a local extinction to sustain the excitation in the coupled system, and therefore to sustain spatiotemporal chaos as long as a local extinction is present. Figure 5(b) shows that the ratio of unstable transverse directions to the total number of transverse directions decreases with increasing coupling strength for a fixed network size.

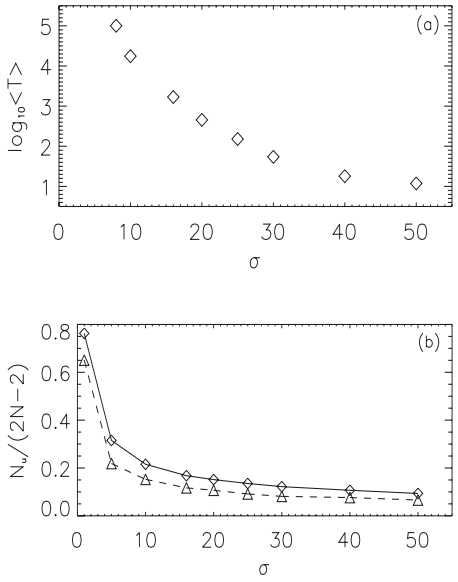

FIG. 5. (a) Average transient lifetime $\langle T\rangle$ vs coupling strength σ for a network of $N=120$ nodes. All the other parameters and simulation procedures are the same as for the GS model in Fig. 3. In a log-log plot, the points for $\sigma \leq 40$ lie approximately on a linear graph. (b) Number of unstable directions normalized to the dimension of the transverse subspace, $N_u/(2N-2)$, vs network size N for the GS model. The full line corresponds to the directions that are unstable somewhere along the excitation cycle, and the dashed line corresponds to the maximum number of unstable directions at a point along the excitation cycle. All the other parameters and simulation procedures are the same as in Fig. 4(b).

B. Transverse modes in the BE model

The BE model shows similar behavior as the GS model regarding the number of unstable transverse modes and the average lifetime of spatiotemporal chaos although the origin of spatiotemporal chaos was reported differently in both systems. Figure 6(a) shows which of the transverse modes are unstable somewhere along the excitation cycle. A comparison with the GS model in Fig. 4(a) reveals that the number of unstable transverse directions is reduced in the BE model for the same coupling strength. Figure 6(b) shows that the total number of unstable transverse directions, $N_u=\Sigma_{k=1}^{N-1}N_u(\kappa)$, increases linearly with the network size N. The rate at which the total number of transverse directions that are unstable somewhere along the excitation cycle grows with the network size N is only slightly larger than the rate at which the maximum number of transverse directions that are unstable at a point along the excitation cycle grows with N. In the BE model the rates dN_u/dN also differ from the rate dT/dN at which the average lifetime of spatiotemporal chaos increases with N.

The results from the BE model are consistent with the qualitative dependence of η and γ in the GS model. From Fig. 3 follows that the rate at which the average lifetime increases with the network size is smaller for the BE model ($\gamma=0.021$) than for the GS model ($\gamma=0.036$) at the same coupling strength σ. The rate η at which the number of unstable transverse directions grow with the network size is also smaller for the BE model ($\eta=0.247$) as it is for the GS model ($\eta=0.332$). This is consistent with the qualitative findings in the GS model for various coupling strengths, where a reduced exponential growth of the average lifetime with network size corresponds to a reduced growth rate of unstable transverse directions with network size. Whether this qualitative relationship can be generalized to other systems exhibiting transient spatiotemporal chaos needs to be addressed in further studies. From the comparison of the GS model with the BE model it follows further that the sum of

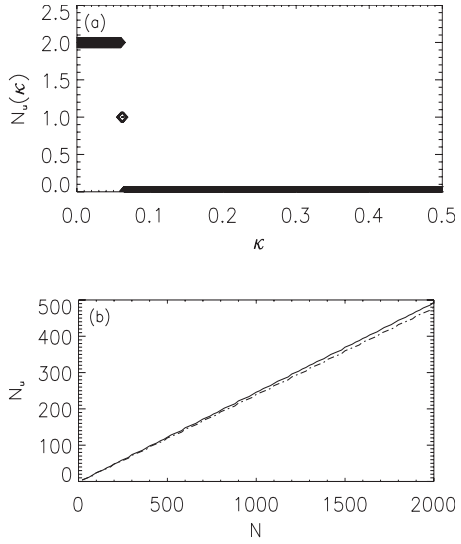

FIG. 6. (a) Maximum number of unstable directions $N_u(\kappa)$ along the excitation cycle for the transverse mode $\kappa=k/N$ in the BE model. Due to the symmetry of the eigenvalues of the Laplacian coupling matrix, $\lambda_k=\lambda_{N-k}$, only $\kappa\leq 0.5$ is plotted. (b) Total number of unstable transverse directions N_u vs network size N in the $2(N-1)$-dimensional transverse subspace of the BE model. The full line corresponds to the total number of directions that are unstable somewhere along the excitation cycle, $N_u=\Sigma_{k=1}^{N-1}N_u(\kappa)$. The dashed line corresponds to the maximum number of unstable directions at a point along the excitation cycle. All the other parameters and simulation procedures are the same as in Fig. 2(b).

all negative Lyapunov exponents transverse to the synchronization manifold is more negative for the GS system than for the BE system. This indicates that the contraction to the synchronization manifold is stronger for the GS system, although the GS system has a longer average lifetime of spatiotemporal chaos. Therefore the sum of the transverse Lyapunov exponents (as calculated in Sec. III) is not a good indicator for the rate at which the average lifetime increases exponentially with N.

V. CONCLUSIONS

Master stability analysis yields insight into the transient nature of spatiotemporal chaos in both systems under study, a regular network of Gray-Scott excitable elements [17] and a regular network of Bär-Eiswirth excitable elements [18]. The origin of spatiotemporal chaos was reported to be different in these two models; a backfiring instability was identified in the Bär-Eiswirth (BE) model [18], and a Šilnikov-like orbit was identified in the Gray-Scott (GS) model [17]. The asymptotic state in both systems is on the invariant synchronization manifold which is characterized by contraction transverse to the manifold everywhere on the attractor. All transverse Lyapunov exponents on the attractor of the synchronization manifold are negative, which is consistent with the collapse of spatiotemporal chaos close to the synchronization manifold.

The average lifetime of transient spatiotemporal chaos typically increases exponentially with the size of the network or medium [2–4,10,13,15]. From the master stability equation it follows that the number of transverse directions that are unstable along a typical excitation cycle, which is a trajectory within the synchronization manifold that is not restricted to the attractor, also increases with the size of the network in the GS model as well as in the BE model. In all simulations (intermodel comparisons and intramodel comparisons) we find that an increase in the rate at which the number of unstable transverse directions grows with the network size corresponds to an increased average transient lifetime for spatiotemporal chaos. Whether this qualitative relationship can be generalized to transient spatiotemporal chaos in other systems needs to be addressed in further studies.

The master stability function [19,20] and its generalization for weighted networks [29] allows us to determine the stability of synchronization in linearly coupled dynamical elements. Further studies will explore whether the asymptotic state in other systems with transient spatiotemporal chaos [2–4,10,13,15] also relates to the attractor on the invariant synchronization manifold, and whether the master stability function which quantifies the stability of transverse perturbations close to the synchronization manifold is a good indicator of the collapse of spatiotemporal chaos.

The analysis of the master stability function will be of further interest in systems where spatiotemporal chaos can be either asymptotic or transient depending on the initial conditions. (i) In a generalization of the GS model, in which two species [instead of one species, Eq. (2)] compete for resource, asymptotic spatiotemporal chaos can be found [30]. Preliminary results show that the transverse Lyapunov exponents on the attractor of the synchronization manifold are negative, which is consistent with numerical simulations in which spatiotemporal chaos was observed to be transient, if the system gets close to the synchronization manifold. Asymptotic spatiotemporal chaos is observed, however, if interfaces develop from species segregation that prevent the system from reaching the neighborhood of the synchronization manifold [30]. (ii) The addition of nonlocal coupling in a regular network of GS-excitable elements can clearly influence the average lifetime of transient spatiotemporal chaos. For a ring network of $N=120$ nodes and two randomly added shortcuts, spatiotemporal chaos was reported to be asymptotic in 70% of the simulations (initial conditions) and transient in 30% of the simulations [15].

ACKNOWLEDGMENT

This research is based upon work supported by the National Science Foundation under Grant No. EPS-0346770.

[1] B. Hof, J. Westerweel, T. M. Schneider, and B. Eckhardt, Nature (London) **443**, 59 (2006).
[2] A. Wacker, S. Bose, and E. Schöll, Europhys. Lett. **31**, 257 (1995).
[3] M. C. Strain and H. S. Greenside, Phys. Rev. Lett. **80**, 2306 (1998).
[4] R. Wackerbauer and K. Showalter, Phys. Rev. Lett. **91**, 174103 (2003).
[5] G. Huber, P. Alstrom, and T. Bohr, Phys. Rev. Lett. **69**, 2380 (1992).
[6] R. Braun and F. Feudel, Phys. Rev. E **53**, 6562 (1996).
[7] F. H. Willeboordse, Phys. Rev. E **47**, 1419 (1993).
[8] Y.-Ch. Lai and R. L. Winslow, Phys. Rev. Lett. **74**, 5208 (1995).
[9] J. P. Crutchfield and K. Kaneko, Phys. Rev. Lett. **60**, 2715 (1988).
[10] A. Politi, R. Livi, G. L. Oppo, and R. Kapral, Europhys. Lett. **22**, 571 (1993).
[11] K. McCann and P. Yodzis, Am. Nat. **144**, 873 (1994).
[12] L. Shulenburger, Y.-Ch. Lai, T. Yalcinkaya, and R. D. Holt, Phys. Lett. A **260**, 156 (1999).
[13] K. Kaneko, Phys. Lett. A **149**, 105 (1990).
[14] R. Wackerbauer and S. Kobayashi, Phys. Rev. E **75**, 066209 (2007).
[15] S. Yonker and R. Wackerbauer, Phys. Rev. E **73**, 026218 (2006).
[16] C. Grebogi, E. Ott, and J. A. Yorke, Physica D **7**, 181 (1983); H. Kantz and P. Grassberger, *ibid.* **17**, 75 (1985); T. Tel, in *Directions in Chaos III*, edited by H. Bai-lin (World Scientific, Singapore, 1990), pp. 149–211.
[17] J. H. Merkin, V. Petrov, S. K. Scott, and K. Showalter, Phys. Rev. Lett. **76**, 546 (1996); J. H. Merkin and M. A. Sadiq, IMA J. Appl. Math. **57**, 273 (1996).
[18] M. Bär and M. Eiswirth, Phys. Rev. E **48**, R1635 (1993).
[19] L. M. Pecora and T. L. Carroll, Phys. Rev. Lett. **80**, 2109 (1998).
[20] M. Barahona and L. M. Pecora, Phys. Rev. Lett. **89**, 054101 (2002).
[21] P. Gray and S. K. Scott, Chem. Eng. Sci. **39**, 1087 (1984).
[22] This diffusion constant $\sigma=16$ in the ring network of coupled Gray-Scott excitable elements corresponds to $D=1$ in the discretized continuous space reaction-diffusion equation [4].
[23] Y. Nishiura and D. Ueyama, Physica D **150**, 137 (2001).
[24] For $N=120$ and $Q=0$ an increase of the ensemble size from 100 to 2000 different randomly chosen initial conditions changed the mean transient time by less than 1% [4].
[25] In [27] it is reported that turbulent patterns are dominant but for not too large systems periodic patterns do exist. In our simulations with three randomly located initial seeds for each simulation we only observed turbulent patterns for all network sizes N under study.
[26] For each data point the frequency distribution of all the transient lifetimes is exponentially decaying, which results in a standard deviation that is of the order of the mean value.
[27] M. Bär, M. Hildebrand, M. Eiswirth, M. Falke, H. Engel, and M. Neufeld, Chaos **4**, 499 (1994).
[28] J. G. Restrepo, E. Ott, and B. R. Hunt, Phys. Rev. Lett. **93**, 114101 (2004).
[29] M. Chavez, D.-U. Hwang, A. Amann, H. G. E. Hentschel, and S. Boccaletti, Phys. Rev. Lett. **94**, 218701 (2005).
[30] R. Wackerbauer, H. Sun, and K. Showalter, Phys. Rev. Lett. **84**, 5018 (2000).